
PSEUDO SPIN-VALVE SWITCH BASED ON FERROMAGNET/SUPERCONDUCTOR/FERROMAGNET TRILAYER MICROBRIDGE.

L. N. Karelina
Institute of Solid State Physics
Russian Academy of Sciences
Chernogolovka, 142432, Russia

V. V. Bolginov *
Institute of Solid State Physics
Russian Academy of Sciences
Chernogolovka, 142432, Russia

Sh. A. Erkenov †
Moscow Institute of Physics and Technology
State University
9 Institutskiy per., Dolgoprudny
Moscow Region, 141700, Russia

S. V. Egorov
Institute of Solid State Physics
Russian Academy of Sciences
Chernogolovka, 142432, Russia

I. Golovchanskiy ‡
Russian National University of Science and Technology (NUST) MISiS
4 Leninsky Prospect, Moscow 119049, Russia

V. I. Chichkov
Russian National University of Science and Technology (NUST) MISiS
4 Leninsky Prospect, Moscow 119049, Russia

A. ben Hamida
Russian National University of Science and Technology (NUST) MISiS
4 Leninsky Prospect, Moscow 119049, Russia

V. V. Ryazanov ‡
Institute of Solid State Physics
Russian Academy of Sciences
Chernogolovka, 142432, Russia

September 2, 2020

ABSTRACT

A noticeable magnetoresistive effect has been observed on ferromagnet/superconductor/ferromagnet (FSF) microbridges based on diluted ferromagnetic PdFe alloy containing as small as 1% magnetic atoms. Microstructuring of the FSF trilayers does not destroy the effect: the most pronounced curves were obtained on the smallest bridges of 6–8 μm wide and 10–15 μm long. Below the superconducting transition we are able to control the critical current of microbridges by switching between P and AP orientations of magnetizations of PdFe layers. The operation of FSF-bridge as a magnetic switch is demonstrated in several regimes providing significant voltage discrimination between digital states or remarkably low bit error rate.

* Also at Skobeltsyn Institute of Nuclear Physics, Lomonosov Moscow State University, Moscow 119991, Russia

† Also at Institute of Solid State Physics, Russian Academy of Sciences, Chernogolovka, 142432, Russia

‡ Also at Moscow Institute of Physics and Technology, State University, 9 Institutskiy per., Dolgoprudny, Moscow Region, 141700, Russia

1 Introduction

At present, development and application of spin-valve devices based on the giant magnetoresistance (GMR) is an intensive field of science and technology (see, for example [1]). Use of a superconducting interlayer (S) between two ferromagnetic metals (F) instead of normal-metal interlayer was proposed in 1999 [2, 3]. ‘Pseudo spin-valve effect’ in FSF-trilayers allows to control superconductivity of a thin superconducting interlayer via mutual orientation of magnetizations M_1 and M_2 in ferromagnetic layers [4–6]. Several different manifestations of the spin-valve effect are discussed. The most straightforward one is based on suppression of superconductivity in F_1SF_2 heterostructures due to spin-ordering antagonism between ferromagnetism and superconductivity. In the case of co-directional M_1 and M_2 orientation (P-orientation) of the outer ferromagnetic layers the superconducting layer critical temperature, T_c , is suppressed due to proximity effect, while in the opposite case (AP-orientation) the F-layer impacts slightly compensate each other and the suppression is weakened [2–6]. A similar effect is observed in the case when both ferromagnetic layers are located on the same side of the superconducting film (SFF structures) [7]. In reality, both the ‘positive’ effect with stronger suppression for P-orientation and the ‘negative’ one with stronger suppression for AP-orientation were observed experimentally depending on the thickness of the ferromagnetic layers [8, 9]. FSF and SFF-structures also demonstrate the triplet spin-valve effect predicted in [9–11] and observed in [12–19] in the case of non-collinear M_1 and M_2 mutual orientations. The magnitude of the T_c suppression due to the triplet spin-valve effect ranges from 0.01 K up to 1.5 K depending on the spin-valve geometry and materials of superconducting and ferromagnetic layers.

Usually the spin-valve effect is observed as peaks or dips of the magnetoresistance at the coercive magnetic fields at which mutual magnetizations of the ferromagnetic layers change. The positive magnetoresistance (i.e. peaks of magnetoresistance) is observed in SF_1F_2 structures due to leakage of the spin-triplet pairs from superconducting layer into the ferromagnetic ones at non-collinear magnetic configurations of the latter’s [14]. FSF type samples usually demonstrate the negative magnetoresistance [4, 6, 12]. Positive magnetoresistance of FSF structures could be caused by stray magnetic fields of domain walls which arise in the coercive magnetic field in the case of large samples [20–22]. To avoid this effect one of the ferromagnetic layers has to be fixed by antiferromagnetic anchor layer (see, for example [6]).

One of the noteworthy aspects of this work is the choice of the material used for ferromagnetic layer deposition. The authors of most previously published works used as the F-layers strong metallic ferromagnets with in-plane magnetizations such as Fe, Ni, Py¹, Co. Rare earth ferromagnets (Ho, Dy) [23] and half-metallic CrO_2 [17] were also applied to observe the spin-valve effect. The weakest ferromagnet was $Cu_{1-x}Ni_x$ alloy ($x \approx 50\%$) with 40–70 K Curie temperature which was used in SFF and SFS structures [5, 14, 19]. Below we demonstrate a noticeable magnetoresistance behavior using very diluted $Pd_{0.99}Fe_{0.01}$ ferromagnet containing as small as 1% at. magnetic atoms. Bulk $Pd_{1-x}Fe_x$ alloy is a ferromagnetic material with long-range ferromagnetic order in the range of Fe concentration $x = 0.001 - 1$ [24, 25]. Strongly diluted compositions with $x = 10^{-6} - 10^{-2}$ undergo the ferromagnetic transition with Curie temperature ranged from 10^{-4} to 35 K [26, 27]. Polycrystalline $Pd_{1-x}Fe_x$ alloys remain ferromagnetic down to the grain sizes of about 10 nm [28]. Thin films of the $Pd_{0.99}Fe_{0.01}$ content with the thickness below 100 nm demonstrate properties of a nanocluster ferromagnet with weak interaction between nanoclusters [29, 30]. At the thickness below 25 nm the interaction between the clusters becomes drastically weaker, because a three-dimensional distribution of the ferromagnetic clusters arising around impurity iron atoms transforms into a two-dimensional one [31, 32]. So the spin-glass magnetic behavior starts to characterize the magnetic response of the films to the external fields [31, 33]. The ferromagnetic-to-paramagnetic state transition occurs at the thickness about of 10 nm [32]. For practical applications it means that thin $Pd_{0.99}Fe_{0.01}$ films possess unique properties of soft magnetic material with weak magnetization values, magnetization reversal in which occurs via independent rotational processes in magnetic nanoclusters with the time $3 - 5 \times 10^{-9}$ s, as it was shown by means of the FMR methods [30].

In this work we study the magnetoresistance of $Pd_{0.99}Fe_{0.01}$ -Nb- $Pd_{0.99}Fe_{0.01}$ trilayer structures (FSF trilayers) in the form of microbridges of different width and length (Fig. 1a). As we will discuss below, microstructuring of the SFS trilayers does not destroy the magnetoresistive effects (Fig. 1b) and allows achieving a high supercurrent density as well as observing resistive switching (Fig. 1d) well below the critical temperature. Due to reduction of the microbridge sizes we also achieve single-domain² magnetic states of ferromagnetic layers and eliminate the noted above effects of the domain structure. The conventional pseudo spin-valve effect on the resistive superconducting transition close to T_c is also investigated as a first step of our experimental study. Based on results obtained in this work we have demonstrated the operation of FSF microbridges as superconducting magnetic memory elements. Low operation temperature allows to amplify additionally the switching effect using non-linear shape of the current-voltage characteristics.

¹Py is $Fe_{20}Ni_{80}$ or close alloy

²more specifically, quasi-uniform

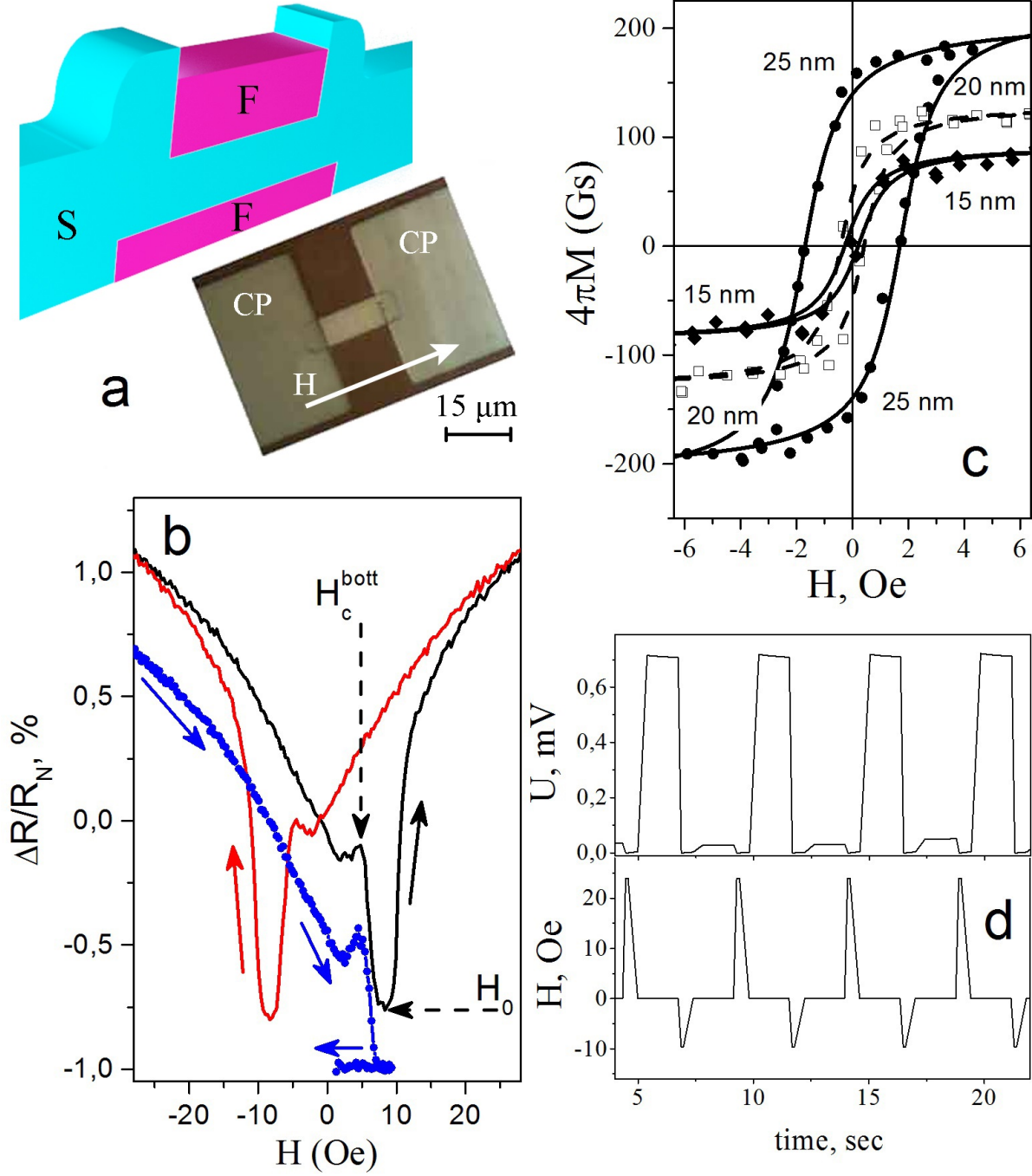


Figure 1: a) A sketch of the FSF sample cross-section and a microphotograph of $8 \times 15 \mu\text{m}^2$ FSF bridge located between the niobium pads (CP). The arrow shows the direction of the external magnetic field. The mark defines the scale in the microphotograph. Definitions of H_c^{bott} and H_0 are given in the text. b) Magnetoresistance of the $6 \times 15 \mu\text{m}^2$ FSF-bridge measured in magnetic field swept from positive to negative values and backward. Solid circles illustrate the magnetic memory effect (see explanation in the text). The difference $R(H)$ to zero-field resistance $R(0)$ normalized on the normal resistance R_N at $T = 4.2$ K is plotted. The temperature is 2.49 K (see Fig. 3). c) Curves of magnetization reversal obtained for $10 \times 10 \mu\text{m}^2$ PdFe layers of different thicknesses using Josephson magnetometry method [34] (see explanation in the text). d) The upper curve: PdFe-Nb-PdFe bridge switching between two “logical states” due to external magnetic field pulses shown below. The temperature is 2.217 K (see Fig. 4a). The bias current is $57 \mu\text{A}$.

2 Samples and experiment

The sample fabrication process starts from the PdFe-Nb-PdFe trilayer deposition on Si/SiO₂ substrate by means of the rf-sputtering for the Pd_{0.99}Fe_{0.01} layers and the magnetron sputtering for the Nb layer. We have studied several series of samples in which thicknesses of top and bottom PdFe layers varied within 45-50 nm and 20-30 nm respectively (see Fig. 1a). All samples showed similar magnetoresistance with aspect ratio related features (see Fig. 2 and a discussion below). The thickness of Nb layer was 15 nm and its critical temperature was strongly affected by the proximity effect from adjacent PdFe layers. More precisely, the critical temperature decreased from 7 K for single Nb film to 2.3-2.6 K for PdFe-Nb-PdFe trilayers while the measured width of the superconducting transition was less than 0.05 K (see Fig. 3b). Then a series of FSF-rectangles of different sizes were formed using the photolithography and argon ion milling. The width w of bridges ranged from 4 μm to 25 μm while the length varied from 14 μm to 108 μm . At the last stage Nb contact pads (CP) were fabricated using the magnetron sputtering followed by the ‘lift-off’ process. The Nb layer was of 120 nm thick and the contact pads were superconducting at all temperatures below 8 K. To ensure good superconducting contact between CP and the central superconducting layer the upper PdFe layer was completely etched during the ion cleaning before the CP deposition. So, the top PdFe layer was shorter by 8 nm due to overlap of the contact pads and the bridge (see Fig. 1a). This value is taken below as a bridge length L .

Our earlier studies [34] show that the Curie temperature T_{Curie} of Pd_{0.99}Fe_{0.01} thin films decreases with thickness due to the percolation nature of the interaction between magnetic clusters [29, 31, 32]. In particular $T_{Curie} \approx 13$ K for 40 nm thick film and $T_{Curie} \approx 9$ K for 25 nm thick film. The same is true for both the coercive fields and saturation magnetization. This is confirmed by our research on SFS and SISFS Josephson junctions based on Pd_{0.99}Fe_{0.01} alloy by means of the Josephson magnetometry method (see [34–36] and Fig. 1c with novel data). Thus, the coercive field for the bottom ferromagnetic layer in the FSF bridges was smaller than for the top one, and gradually reversing the magnetic field from large positive value to negative one it was possible to achieve antiparallel magnetization configuration in some range of negative magnetic fields. In this field range one could expect the resistance reduction due to decrease of the total spin-polarized electron diffusion into the S-layer. Any antiferromagnetic anchor layers were not used to fix the magnetization of one of the ferromagnetic layers as it was done in earlier works [6, 8, 12–14] since it could enhance the exchange interaction in PdFe layer. In addition, this is not necessary in our case because the distorting stray-field effects [20–22] are not occurred when using the weakly ferromagnetic PdFe alloy.

We started with the usual spin-valve effect study using magnetoresistance measurements of FSF-bridges of different sizes at various temperatures within the superconducting transition region. Experiments were done in ⁴He cryostat equipped by a membrane pressure stabilizer that allowed to fix the temperature with an accuracy better than 0.01 K during the experiment. In Fig. 1b we present a typical magnetoresistive curve $\Delta R(H)$, where $\Delta R = R(H) - R(0)$ and the magnetic field H is applied in plane parallel to the long side of the bridge (see Fig. 1a) by a superconducting solenoid. We start from large positive magnetic field H , which is much larger the saturation one for both F layers, and sweep H to large negative values and back. One can clearly see a sharp decrease of the magnetoresistance at two magnetic fields $\pm H_0$ opposite in sign to the initial saturated magnetizations. Let us consider in more details the magnetization reversal as the external magnetic field H changes from large negative (-30 Oe) to large positive ($+30$ Oe) values. At $H = -30$ Oe both PdFe layers are magnetized in the same (negative) direction. As H reaches some small positive value the thin (bottom) layer starts to turn its magnetization in the positive direction. At first, the initial magnetic ordering disappears completely at the coercive field for the bottom layer $H = H_c^{bot}$ (see definition in Figs. 1b, 2) resulting in stray magnetic fields and positive magnetoresistance, as discussed in [20, 22]. This is seen in Fig. 1b and Fig. 2 as a small rise in magnetoresistance near H_c^{bot} . Further reorientation of local magnetic moments in bottom F-layer in positive direction causes a sharp decrease in the magnetoresistance. The main effect of the negative magnetoresistance is obviously due to decrease of the total spin-polarized electron diffusion into the S-layer at AP-orientation of F-layers since this is the only possible mechanism mentioned in introduction providing a negative magnetoresistance in FSF-trilayers. As soon as the thick top F-layer starts to reverse its magnetization (at $H \approx +H_0$ in Figs. 1b and 2), the magnetoresistance begins to rise. In higher fields, the magnetoresistance increases approximately as H^2 in accordance with the Ginzburg-Landau theory (see, for example, [37]).

The next step was to study the effect of the bridge length and aspect ratio on the magnetoresistive curves. The most pronounced dips were observed for the smallest samples of 4 – 20 μm long and 6 – 8 μm wide. As dimensions of the bridge increased these dips became wider and gradually merged with the magnetoresistive curve, appearing as small distortions. We believe this blurring of the effect related to mutual F-layer magnetizations is due to domain structure (more precisely – a long-range magnetic inhomogeneity [32, 33]) of the long PdFe strips. This is consistent with our earlier studies [34] which reveal a crossover from quasi-uniform to non-uniform magnetic state as the PdFe film size increase from $10 \times 10 \mu\text{m}^2$ to $30 \times 30 \mu\text{m}^2$.

The effect magnitude increases as the sample superconducting state strengthens when temperature decrease at the region of the resistive transition. In Fig. 3 we present the superconducting resistive transition and a series of magnetoresistive

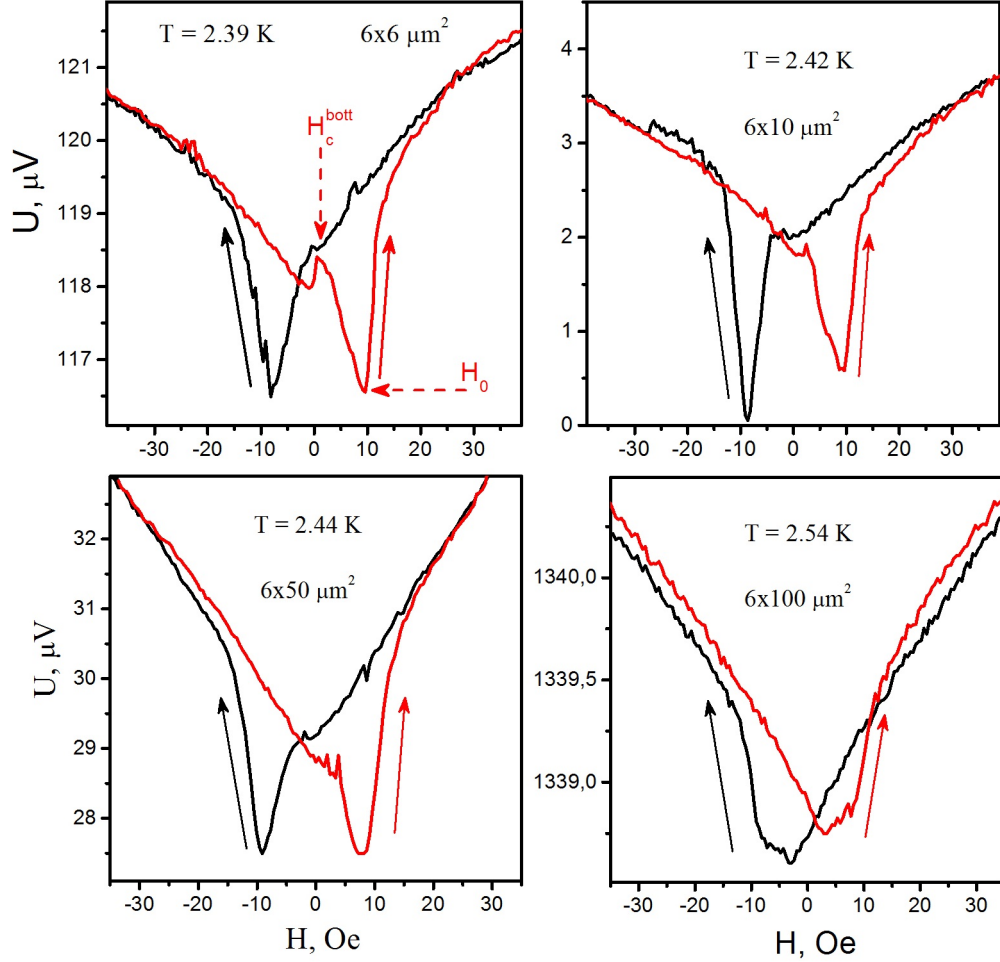


Figure 2: The magnetoresistance of FSF bridges with the same F-layer width $6\mu\text{m}$ and different length and aspect ratio. The length is represented for the top PdFe layer. The thickness of the top PdFe layer is 45 nm and of the bottom PdFe layer is 25 nm. Definitions of H_c^{bott} and H_0 are given in the text. The bias current is $20\mu\text{A}$.

curves obtained for $6 \times 15 \mu\text{m}^2$ bridge at various temperatures within the resistive transition $T_c^{(e)} < T < T_c^{(b)}$.³ The absolute magnitude of the effect increases from 0.05Ω to 0.3Ω , which corresponds to the resistance change up to 5% relative to the normal state resistance and up to 70% relative to the resistance at zero magnetic field at the corresponding temperature. At the $T = 2.55 \text{ K} \approx T_c^{(b)}$ the dip depth is about 0.04Ω which is about 0.6% to the normal state resistance (Fig. 3a). As the temperature decreases by 0.02 K the effect increases by 2.5 times (Fig. 3c). At $T = 2.51 \text{ K}$ two thirds of the resistive transition already passed and the maximum dip depth of 0.14Ω is achieved which corresponds to 2% of normal state resistance. At lowest temperature $T = 2.49 \text{ K} \approx T_c^{(e)}$ the effect slightly decreases since the bridge have a zero resistance in a vicinity of H_0 . The spin-valve effect was evaluated in terms of the critical temperature variation in [4–6, 8, 12–17]. We roughly estimate that the dip in magnetoresistive curve at $T = 2.49 \text{ K}$ is equivalent to the critical temperature change of about 1 mK. So small change is hardly possible to observe doing $R(T)$ measurement, but we were able to detect it on $R(H)$ curves in our experimental situation. The relative effect magnitude normalized on the zero-field resistance at given temperature rises from 0.6% at $T = T_c^b$ to 90% at $T = T_c^e$. The temperature dependence additionally confirms that the magnetoresistive effect is due to enhance of the superconductivity of the niobium film rather than PdFe anomalous magnetoresistance, for example.

³Here $T_c^e = 2.55 \text{ K}$ and $T_c^b = 2.49 \text{ K}$ denote the end and the beginning of the superconducting transition and are introduced for clarity.

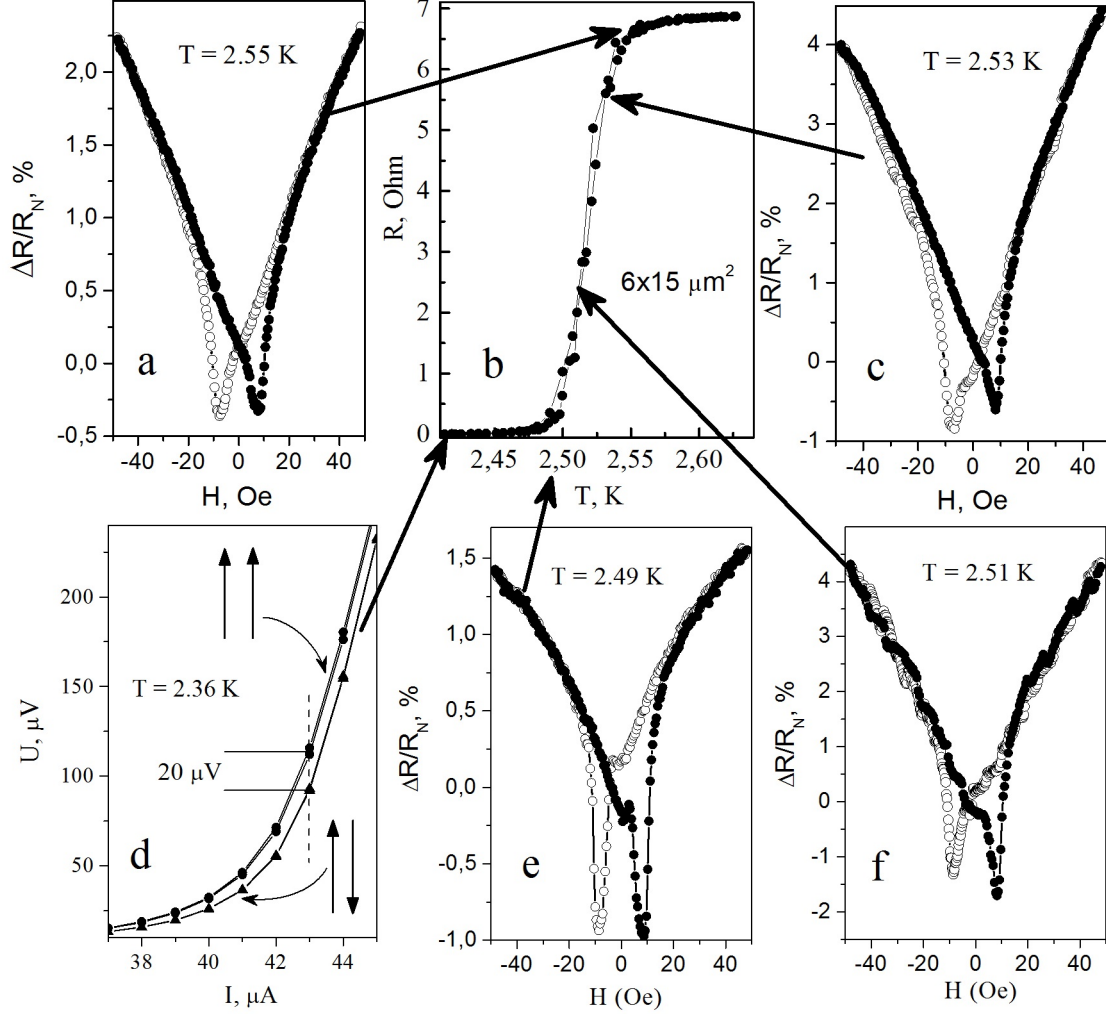


Figure 3: a,c,e,f) Magnetoresistance obtained at different temperatures within the superconducting transition for $6 \times 15 \mu\text{m}^2$ bridge. The difference $R(H)$ to zero-field resistance $R(0)$ normalized on the normal resistance R_N at $T = 4.2$ K is plotted. The bias current is $20 \mu\text{A}$. b) Superconducting transition of the $6 \times 15 \mu\text{m}^2$ sample. d) IV curves for parallel and anti-parallel orientations at $T = 2.36$ K zoomed in near the critical current.

It is important to note that investigated samples demonstrate a magnetoresistive memory effect. In the experiments discussed above the magnetic field is swept from large positive value to large negative one and backward. In the measurement represented by the blue line and symbols at the bottom of Fig. 1b we have reversed the backward sweep at $H_r = H_0$ and gradually decreased magnetic field to zero. In this case the magnetoresistance remains stable down to the negative field value corresponding to destruction of the AP state. Note that the sweep can be reversed at any magnetic field H_r within the dip with some observed memory effect, however the most pronounced effect takes place if $H_r = H_0$. This fact additionally confirms that the effect is due to the steady AP configuration of the ferromagnetic layer mutual magnetization and this allows to use our FSF trilayers as superconducting logic elements.

Below the superconducting transition ($T < T_c^e$), the current-voltage characteristics of the microbridges cease to be linear and acquire a region of zero resistance at $I < I_c$ (Fig. 4a). Magnetoresistive curves similar to those shown in Figs. 3a,c,e,f can also be observed at these temperatures if the bias current is slightly above I_c . We also found that below T_c^e the effect of mutual magnetization of ferromagnetic layers is to be described in terms of the critical current change (Fig. 3d). The ability to control the critical current expands the working temperature range of the spin-valves based on the FSF-microbridges and gives the advantage compared to conventional FSF spin-valve structures [4–19] operating in a narrow temperature range near the superconducting transition. The temperature dependence of the critical current for SFS bridge with AP mutual F-layer magnetizations obeys the well-known $(1 - T/T_c)^{3/2}$ law for thin film depairing

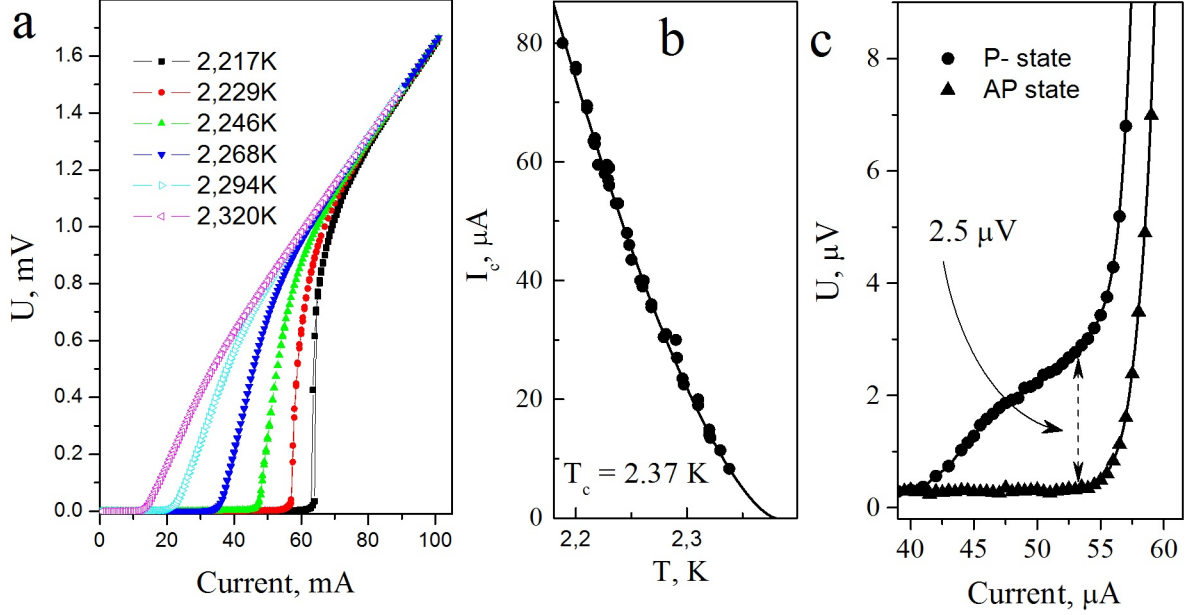


Figure 4: a) The evolution of IV curves with the temperature in the superconducting states. b) The temperature dependence of the sample critical current. The line shows approximation by $(1 - T/T_c)^{3/2}$ dependence. c) IV curves for parallel and anti-parallel orientations at $T = 2.217$ K zoomed in near the critical current.

current (see Fig. 4b). A shape of the IV characteristic transforms steadily from a linear curve at $T = T_c^e$ to highly nonlinear one with a zero-resistance region and a sharp hopping into resistive state similar to that in [38]. In Fig. 4a the latter occurs at $T = 0.93T_c$ ($T = 2.2$ K), where $T_c \approx 2.37$ K was determined as the fitting parameter in Fig. 4b. At lower temperatures IV curves demonstrate hysteretic behavior due to sample overheating in the resistive state. Moreover, the hopping is driven mainly by noise and a reproducible switching between the normal and the superconducting states is not possible. At intermediate temperatures IV -curves for both P and AP orientations are single-valued and one can control the voltage on the sample via the mutual orientation of PdFe magnetizations.

We are interested in maximal voltage difference between AP and P ‘digital states’, which makes it easier to detect logical switching of the memory element, increases the corresponding Josephson frequency (i.e. readout rate) and determines a possible integration of the element into superconducting digital RSFQ-circuitry. This difference increases at lower temperatures due to increasing non-linearity of IV -curves (Fig. 4a). The maximum voltage difference about $600\mu\text{V}$ (Fig. 1d) was obtained close to the boundary temperature (at $T = 2.217$ K in Fig. 4a). At this temperature range on the IV curve a resistive region appears for P state in which the voltage changes quite smoothly with the current in the same range, where the AP state is superconducting (Fig. 4c). For the bias current marked with an arrow in the Fig. 4c we can obtain a reproducible switching between $2.5\mu\text{V}$ and, in fact, the superconducting state ($U = 0$). In other words, the magnetoresistance ratio $(R_P - R_{AP})/R_{AP}$ is infinitely large. In Fig. 1d switches between $700\mu\text{V}$ and $25\mu\text{V}$ voltage levels are represented with magnetoresistance ratio equal 27. The low voltage level in the resistive state of the FSF bridges eliminates overheating and completely avoids accidental switching. The width of the low-voltage region, which reaches 30% of the critical current, provides large bias current margins. The origin of the smooth low-voltage region is not entirely clear now but it is undoubtedly very important for applications.

3 Discussion

In this paper we propose new FSF memory elements in the form of microbridges and we would like to discuss their advantages and disadvantages compared to unstructured FSF spin-valve devices. The result shown in Fig. 1d and Fig. 4c reliably proves that the memory effect can manifest itself in FSF microbridges noticeably below T_c and use of the PdFe-Nb-PdFe microbridges as memory elements is still possible at low temperatures, not just in the superconducting transition region. The idea to control the critical current rather than the critical temperature was proposed firstly in the work by A. Rusanov et al [38]. This approach distinguishes [38] and this work from the most of previous ones in which FSF trilayers have not been structured and only measurements in the range of the resistive transition were

possible. Surprisingly we have found only few works studying superconductor-ferromagnet microbridges [20, 21, 38] and demonstrating positive magneto-resistive effects related to remagnetization of F-layers. The use of a very weak ferromagnet makes it possible to observe a distinct negative magnetoresistance effect, which is not distorted by the magnetostatic interaction of the layers during the sample magnetization reversal. It was shown in [6, 8, 12–14] that an anchor anti-ferromagnetic layer is a key element to observe the spin-valve effect using traditional ferromagnets (for example, Py). The cluster nature of the PdFe magnetism allows the magnetic field lines to close inside the ferromagnetic film, which reduces the domain formation, weakens stray fields and the magnetostatic interaction as a whole. The use of the “cryogenic” ferromagnet also provided a fairly wide transition area between the resistive and superconducting regions, which allowed us to study the evolution of the shape of current-voltage characteristics, to find conditions for zero resistance in a low-voltage state and maximum voltage amplitude of magnetic switching.

The results obtained are important primarily for development of the Josephson magnetic memory. In earlier works of our group [34–36] digital states of Josephson memory elements were determined by values of the magnetization flux through the cross-section of the multilayered SFS or SISFS junctions, which resulted from the remagnetization of a single PdFe thin layer. This type of Josephson memory elements is hardly to be scalable since the magnetic flux vanishes with the junction sizes. On the contrary, FSF bridges can decrease almost unlimitedly, down to deeply submicron-scale sizes. The enhancement of the detected memory effect can be achieved using PdFe-Nb-PdFe heterostructures as a Josephson barrier in multilayer Josephson S-(F1sF2)-S junctions [39]. The high transparency of the diluted Pd_{0.99}Fe_{0.01} alloy for the Josephson supercurrent is an important advantage for use in these devices.

To conclude, in the present paper magnetoresistive characteristics and switches between superconducting and resistive state of trilayer FSF (Pd_{0.99}Fe_{0.01}-Nb-Pd_{0.99}Fe_{0.01}) bridges were studied. Despite of very low content of magnetic atoms in Pd_{0.99}Fe_{0.01} resulting in low Curie temperature we have observed noticeable negative magnetoresistance at antiparallel orientation of magnetizations of PdFe layers in the FSF structures. At temperatures noticeably lower than the resistive transition to the superconducting state the change of the F-layers mutual magnetization allows to control the critical current of the SFS microbridges. This provides a demonstration of the magnetic memory effect with switching between superconducting (or low-voltage) state and resistive state with the voltage change up to 0.6 mV. An important advantage of FSF microbridges in comparison with Josephson SFS memory previously proposed is the ability to reduce these structures down to deeply submicron-scale sizes.

The work is published under support of RFBR grant No. 19–32–90162.

References

- [1] E. Y. Tsymbal and D. G. Pettifor. Perspectives of giant magnetoresistance. In H. Ehrenreich and F. Spaepen, editors, *Solid State Physics - Advances in Research and Applications*, volume 56, pages 113–237. Academic Press, 2001.
- [2] L. R. Tagirov. Low-field superconducting spin switch based on a superconductor/ferromagnet multilayer. *Physical Review Letters*, 83:2058–2061, 1999.
- [3] A. I. Buzdin, A. V. Vedyayev, and N. V. Ryzhanova. Spin-orientation – dependent superconductivity in F / S / F structures. *Europhysics Letters*, 48:686, 1999.
- [4] G. Deutscher and F. Meunier. Coupling Between Ferromagnetic Layers Through a Superconductor. *Physical Review Letters*, 22(9):395–396, 1969.
- [5] J. Y. Gu, Chun Yeol You, J. S. Jiang, and S. D. Bader. Magnetization-orientation dependence of the superconducting transition temperature and magnetoresistance in the ferromagnet-superconductor-ferromagnet trilayer system: CuNi/Nb/CuNi. *Physical Review Letters*, 89:267001, 2002.
- [6] Ion C. Moraru, W. P. Pratt, and Norman O. Birge. Magnetization-dependent T_c shift in ferromagnet/superconductor/ferromagnet trilayers with a strong ferromagnet. *Physical Review Letters*, 96:037004, 2006.
- [7] Sangjun Oh, D. Youm, and M. R. Beasley. A superconductive magnetoresistive memory element using controlled exchange interaction. *Applied Physics Letters*, 71:2376–2378, 1997.
- [8] P. V. Leksin, N. N. Garif’yanov, I. A. Garifullin, J. Schumann, V. Kataev, O. G. Schmidt, and B. Büchner. Physical properties of the superconducting spin-valve Fe/Cu/Fe/In heterostructure. *Physical Review B*, 85:024502, 2012.
- [9] Ya. V. Fominov, A. A. Golubov, T. Yu. Karminskaya, M. Yu. Kupriyanov, R. G. Deminov, and L. R. Tagirov. Superconducting triplet spin valve. *JEPT Lett.*, 91:308–313, 2010.
- [10] Ya V. Fominov, A. A. Golubov, and M. Yu Kupriyanov. Triplet proximity effect in FSF trilayers. *Journal of Experimental and Theoretical Physics Letters*, 77:510–515, 2003.

- [11] T. Yu Karminskaya, A. A. Golubov, and M. Yu Kupriyanov. Anomalous proximity effect in spin-valve superconductor/ferromagnetic metal/ferromagnetic metal structures. *Physical Review B*, 84:064531, 2011.
- [12] Jian Zhu, Ilya N. Krivorotov, Klaus Halterman, and Oriol T. Valls. Angular dependence of the superconducting transition temperature in ferromagnet-superconductor-ferromagnet trilayers. *Physical Review Letters*, 105:207002, 2010.
- [13] P. V. Leksin, N. N. Garif'yanov, I. A. Garifullin, Ya V. Fominov, J. Schumann, Y. Krupskaya, V. Kataev, O. G. Schmidt, and B. Büchner. Evidence for triplet superconductivity in a superconductor-ferromagnet spin valve. *Physical Review Letters*, 109:057005, 2012.
- [14] V. I. Zdravkov, J. Kehrle, G. Obermeier, D. Lenk, H. A. Krug Von Nidda, C. Müller, M. Yu Kupriyanov, A. S. Sidorenko, S. Horn, R. Tidecks, and L. R. Tagirov. Experimental observation of the triplet spin-valve effect in a superconductor-ferromagnet heterostructure. *Physical Review B*, 87:144507, 2013.
- [15] X. L. Wang, A. Di Bernardo, N. Banerjee, A. Wells, F. S. Bergeret, M. G. Blamire, and J. W.A. Robinson. Giant triplet proximity effect in superconducting pseudo spin valves with engineered anisotropy. *Physical Review B*, 89:140508, 2014.
- [16] Alejandro A. Jara, Christopher Safranski, Ilya N. Krivorotov, Chien Te Wu, Abdul N. Malmi-Kakkada, Oriol T. Valls, and Klaus Halterman. Angular dependence of superconductivity in superconductor/spin-valve heterostructures. *Physical Review B*, 89:184502, 2014.
- [17] A. Singh, S. Voltan, K. Lahabi, and J. Aarts. Colossal proximity effect in a superconducting triplet spin valve based on the half-metallic ferromagnet CrO_2 . *Physical Review X*, 5:021019, 2015.
- [18] M. G. Flokstra, T. C. Cunningham, J. Kim, N. Satchell, G. Burnell, P. J. Curran, S. J. Bending, C. J. Kinane, J. F.K. Cooper, S. Langridge, A. Isidori, N. Pugach, M. Eschrig, and S. L. Lee. Controlled suppression of superconductivity by the generation of polarized Cooper pairs in spin-valve structures. *Physical Review B*, 91:060501, 2015.
- [19] D. Lenk, R. Morari, V. I. Zdravkov, A. Ullrich, Yu Khaydukov, G. Obermeier, C. Müller, A. S. Sidorenko, H. A.Krug Von Nidda, S. Horn, L. R. Tagirov, and R. Tidecks. Full-switching FSF-type superconducting spin-triplet magnetic random access memory element. *Physical Review B*, 96:184521, 2017.
- [20] V V Ryazanov, V A Oboznov, A S Prokof'ev, and S V Dubonos. Proximity effect and spontaneous vortex phase in planar SF structures. *Journal of Experimental and Theoretical Physics Letters*, 77:39–43, 2003.
- [21] A. Yu Rusanov, M. Hesselberth, J. Aarts, and A. I. Buzdin. Enhancement of the superconducting transition temperature in Nb/permalloy bilayers by controlling the domain state of the ferromagnet. *Physical Review Letters*, 93:057002, 2004.
- [22] Tae-Jong Hwang and Dong Ho Kim. Influence of stray fields and the proximity effect in ferromagnet/superconductor/ferromagnet spin valves. *Journal of the Korean Physical Society*, 61:1628–1632, 2012.
- [23] Yuanzhou Gu, Gábor Halász, J. W.A. Robinson, and M. G. Blamire. Large Superconducting Spin Valve Effect and Ultrasmall Exchange Splitting in Epitaxial Rare-Earth-Niobium Trilayers. *Physical Review Letters*, 115:067201, 2015.
- [24] B. Heller, K. H. Speidel, R. Ernst, A. Gohla, U. Grabow, V. Roth, G. Jakob, F. Hagelberg, J. Gerber, S. N. Mishra, and P. N. Tandon. Transient field measurement in the giant moment PdFe alloy. *Nuclear Instruments and Methods in Physics Research B*, 142:133–138, 1998.
- [25] J. Crangle and W. R. Scott. Dilute ferromagnetic alloys. *Journal of Applied Physics*, 36:921–928, 1965.
- [26] C. Büscher, T. Auerswald, E. Scheer, A. Schröder, H. V. Löhneysen, and H. Claus. Ferromagnetic transition in dilute Pd-Fe alloys. *Physical Review B*, 46:983–989, 1992.
- [27] R P Peters, Ch. Buchal, M Kubota, R M Mueller, and F Pobell. Palladium-Iron: A Giant-Moment Spin-Glass at Ultralow Temperatures. *Physical Review Letters*, 53(11):1108–1111, 1984.
- [28] T Shinohara, T Sato, T Taniyama, and I Nakatani. Size dependent magnetization of PdFe fine particles. *Journal of Magnetism and Magnetic Materials*, 196-197:94–95, 1999.
- [29] L. S. Uspenskaya, A. L. Rakhmanov, L. A. Dorosinskii, A. A. Chugunov, V. S. Stolyarov, O. V. Skryabina, and S. V. Egorov. Magnetic patterns and flux pinning in $\text{Pd}_{0.99}\text{Fe}_{0.01}$ -Nb hybrid structures. *JETP Letters*, 97:155–158, 2013.
- [30] I. A. Golovchanskiy, V. V. Bolginov, N. N. Abramov, V. S. Stolyarov, A. Ben Hamida, V. I. Chichkov, D. Roditchev, and V. V. Ryazanov. Magnetization dynamics in dilute $\text{Pd}_{1-x}\text{Fe}_x$ thin films and patterned microstructures considered for superconducting electronics. *Journal of Applied Physics*, 120:163902, 2016.

- [31] V. V. Bol'ginov, O. A. Tikhomirov, and L. S. Uspenskaya. Two-component magnetization in Pd_{0.99}Fe_{0.01} thin films. *JETP Letters*, 105:169–173, 2017.
- [32] L S Uspenskaya, A L Rakhmanov, L A Dorosinskii, S I Bozhko, V S Stolyarov, and V V Bolginov. Magnetism of ultrathin Pd_{0.99}Fe_{0.01} films grown on niobium. *Materials Research Express*, 1:036104, 2014.
- [33] L. S. Uspenskaya and I. N. Khlyustikov. Anomalous magnetic relaxation in thin Pd_{0.99}Fe_{0.01} films. *Journal of Experimental and Theoretical Physics*, 125:875–878, 2017.
- [34] V. V. Bol'ginov, V. S. Stolyarov, D. S. Sobanin, A. L. Karpovich, and V. V. Ryazanov. Magnetic switches based on Nb-PdFe-Nb Josephson junctions with a magnetically soft ferromagnetic interlayer. *JETP Letters*, 95:366–371, 2012.
- [35] Timofei I. Larkin, Vitaly V. Bol'ginov, Vasily S. Stolyarov, Valery V. Ryazanov, Igor V. Vernik, Sergey K. Tolpygo, and Oleg A. Mukhanov. Ferromagnetic Josephson switching device with high characteristic voltage. *Applied Physics Letters*, 100:222601, 2012.
- [36] S. V. Bakurskiy, N. V. Klenov, I. I. Soloviev, V. V. Bolginov, V. V. Ryazanov, I. V. Vernik, O. A. Mukhanov, M. Yu Kupriyanov, and A. A. Golubov. Theoretical model of superconducting spintronic SIsFS devices. *Applied Physics Letters*, 102(19):192603, 2013.
- [37] V. V. Schmidt. *The Physics of Superconductors (Section 3.5)*. Springer-Verlag, 1997.
- [38] A. Rusanov, M. Hesselberth, S. Habraken, and J. Aarts. Depairing currents in superconductor ferromagnet Nb/CuNi trilayers close to T_c. *Physica C*, 404:322–325, 2004.
- [39] Nikolay Klenov, Yury Khaydukov, Sergey Bakurskiy, Roman Morari, Igor Soloviev, Vladimir Boian, Thomas Keller, Mikhail Kupriyanov, Anatoli Sidorenko, and Bernhard Keimer. Periodic Co / Nb pseudo spin valve for cryogenic memory. *Beilstein Journal of Nanotechnology*, 10:833–839, 2019.